Redox Biology 37 (2020) 101742

Contents lists available at ScienceDirect

Redox Biology

journal homepage: www.elsevier.com/locate/redox

Research Paper

Homocysteine promotes hepatic steatosis by activating the adipocyte lipolysis in a HIF1α-ERO1α-dependent oxidative stress manner

Yu Yan [a], Xun Wu [b,c], Pengcheng Wang [a], Songyang Zhang [a], Lulu Sun [a], Yang Zhao [d], GuangYi Zeng [a], Bo Liu [a], Guoheng Xu [a], Huiying Liu [a], Lei Wang [b,c,**], Xian Wang [a,***], Changtao Jiang [a,e,f,*]

[a] Department of Physiology and Pathophysiology, School of Basic Medical Sciences, Peking University, Key Laboratory of Molecular Cardiovascular Science, Ministry of Education, Beijing, 100191, PR China
[b] National Laboratory of Biomacromolecules, CAS Center for Excellence in Biomacromolecules, Institute of Biophysics, Chinese Academy of Sciences, Beijing, 100101, PR China
[c] College of Life Sciences, University of Chinese Academy of Sciences, Beijing, 100049, PR China
[d] Department of Laboratory Medicine, Peking University Third Hospital, Beijing, 100191, PR China
[e] Center of Basic Medical Research, Institute of Medical Innovation and Research, Third Hospital, Peking University, Beijing, 100191, PR China
[f] Center for Obesity and Metabolic Disease Research, School of Basic Medical Sciences, Peking University, Beijing, 100191, PR China

ARTICLE INFO

Keywords:
Hyperhomocysteinemia
Nonalcoholic fatty liver
Adipocyte lipolysis
ER oxidoreductin 1α
Hypoxia-inducible factor 1α

ABSTRACT

Hyperhomocysteinemia (HHcy) is related to liver diseases, such as nonalcoholic fatty liver (NAFL). Although the precise pathogenesis of NAFL is still largely unknown, the links between organs seem to play a vital role. The current study aimed to explore the role of white adipose tissue in homocysteine (Hcy)-induced NAFL. Blood samples from nonhyperhomocysteinemia or hyperhomocysteinemia individuals were collected to assess correlation between Hcy and triglyceride (TG) or free fatty acids (FFAs) levels. C57BL/6 mice were maintained on a high-methionine diet or administered with Hcy (1.8 g/L) in the drinking water to establish an HHcy mouse model. We demonstrated that Hcy activated adipocyte lipolysis and that this change was accompanied by an increased release of FFAs and glycerol. Excessive FFAs were taken up by hepatocyte, which resulted in lipid accumulation in the liver. Treatment with acipimox (0.08 g kg^{-1} day^{-1}), a potent chemical inhibitor of lipolysis, markedly decreased Hcy-induced NAFL. Mechanistically, hypoxia-inducible factor 1α (HIF1α)-endoplasmic reticulum oxidoreductin 1α (ERO1α) mediated pathway promoted H_2O_2 accumulation and induced endoplasmic reticulum (ER) overoxidation, ER stress and more closed ER-lipid droplet interactions, which were responsible for activating the lipolytic response. In conclusion, this study reveals that Hcy activates adipocyte lipolysis and suggests the potential utility of targeted ER redox homeostasis for treating Hcy-induced NAFL.

1. Introduction

Non-alcoholic fatty liver disease (NAFLD) is the most common chronic liver disease, which comprises a disease spectrum of liver conditions ranging from simple steatosis to nonalcoholic steatohepatitis, characterized by more advanced cirrhosis and hepatocellular cancer [1]. A pathological feature of nonalcoholic fatty liver (NAFL) development is the accumulation of triglyceride (TG) in hepatocytes [2]. Although the precise pathogeneses of NAFL and lipid droplet (LD) formation are still poorly understood, the links between organs appear to play a crucial role [3].

Homocysteine (Hcy) is a toxic sulfur-containing non-constitutive amino acid derived from the metabolism of the essential amino acid methionine. Elevated plasma Hcy levels (>15 μM) are defined as hyperhomocysteinemia (HHcy), and Hcy levels are higher in patients with NAFLD [4]. HHcy has been established as an independent risk

* Corresponding author. Department of Physiology and Pathophysiology, School of Basic Medical Sciences, Peking University, Key Laboratory of Molecular Cardiovascular Science, Ministry of Education, Beijing, 100191, PR China.
** Corresponding author. National Laboratory of Biomacromolecules, CAS Center for Excellence in Biomacromolecules, Institute of Biophysics, Chinese Academy of Sciences, Beijing, 100101, PR China.
*** Corresponding author.
E-mail addresses: wanglei@ibp.ac.cn (L. Wang), xwang@bjmu.edu.cn (X. Wang), jiangchangtao@bjmu.edu.cn (C. Jiang).

https://doi.org/10.1016/j.redox.2020.101742
Received 20 January 2020; Received in revised form 25 September 2020; Accepted 28 September 2020
Available online 1 October 2020

factor for cardiovascular disease in humans [5]. The epidemiological literature also indicates that HHcy is associated with insulin resistance and which is considered a chronic inflammatory status [6,7]. Previously, we have showed that Hcy induces insulin resistance in mice by regulating the expression and secretion of resistin from adipose tissue [8]. Moreover, we demonstrate that Hcy induces adipose tissue endoplasmic reticulum (ER) stress and then provokes adipose inflammation, affecting insulin sensitivity [9]. The above evidence suggests that abnormal Hcy metabolism leads to dysregulation of adipose tissue, but the role of adipose tissue and the underlying mechanism in Hcy-induced hepatic lipid accumulation remains largely unknown.

White adipose tissue (WAT) is a major energy repository that regulates the storage and breakdown of TG. Excess nutrients are converted to TG and stored as LDs in adipocytes [2]. On demand, TG is hydrolyzed by lipases to free fatty acids (FFAs) and glycerol in a process termed lipolysis for energy production [10]. Only adipocytes have the ability to mobilize their fat stores and release FFAs into the circulation to supply energy for the needs of other organs [11]. However, when this balance is perturbed, dysregulation of adipose tissue TG metabolism may result in elevated levels of circulating FFAs, which has profound effects on systemic metabolic homeostasis [12]. An uncontrolled lipolytic response leads to ectopic deposition of lipids and metabolic dysfunction due to lipotoxic effects. Excessive exposure and uptake of FFAs in nonadipose tissue may be a major contributor to metabolic diseases such as NAFLD, obesity and type 2 diabetes [13].

Accumulating evidence suggest that intracellular oxidative stress and ER stress can initiate lipolytic responses in WAT, leading to subsequent lipotoxicity and dyslipidemia [14,15]. Inside the cell, the ER is an organelle that synthesizes, folds, and transports proteins. However, accumulation of unfolded oxidative proteins accompanied by abnormal disulfide bond generation in the ER lumen causes ER stress [16,17]. The folding process of oxidized proteins is regulated by a series of enzymes in the ER. ERO1α (ER oxidoreductin 1α), an ER-specific sulfhydryl oxidase, is the main source of *de novo* generated disulfide bonds. ERO1α utilizes molecular oxygen to generate disulfide and H_2O_2, and mediates the oxidative protein folding via protein disulfide isomerase [18]. Oxidative protein folding is a source of cellular oxidative stress [17]. Indeed, ERO1α may be an important contributor causing cellular oxidative stress, and 25% of intracellular reactive oxygen species (ROS) production during protein synthesis is mediated by ERO1α [17]. The excessive production of ROS in cells will provoke the oxidation of DNA and proteins. There is evidence that hyperactivation of ERO1α is accompanied by the occurrence of ER stress [19]. Therefore, the regulation of ERO1α is particularly crucial for preventing ER overoxidation and stress.

In general, hypoxia is an important source of ER oxidative stress and ER stress [20,21]. Hypoxia-inducible factor 1 (HIF1), a nuclear transcription factor, is stable under hypoxic conditions. HIF functions as an oxygen-sensitive HIF1α subunit and constitutively expressed β-subunit (ARNT or HIF1β) [22]. Our previous research shows that HIF1α can regulate insulin resistance in adipose tissue, and inhibiting HIF1α increases insulin sensitivity and reduces insulin resistance [23]. Hypoxia is also a major source of cellular oxidative stress. Our recent finding suggests that HIF1α can regulate ERO1α transcription in endothelial cells [24], but the mechanism involved in ER peroxidation and stress in adipose tissue is still an open question.

In this study, we reported that Hcy-induced ectopic lipid deposition in the liver is due to uncontrolled adipose tissue lipolysis. Besides, ER redox homeostasis is associated with the lipolysis response involving the HIF1α-ERO1α pathway, which is a novel mechanism of Hcy-induced lipolytic process.

2. Materials and methods

2.1. Reagents and antibodies

L-Homocysteine (Hcy, H4628), acriflavine (ACF, HY-100575) and acipimox (A7856) were purchased from Sigma-Aldrich (St. Louis, MO, USA). The following antibodies were used in this work: anti-ERO1α (MABT376) antibody was purchased from Merck Millipore (Darmstadt, Germany). Anti-HIF1α (20960-1-AP, RRID:AB_10732601) and anti-Rab18 (60057–1-Ig, RRID:AB_2173930) antibodies were purchased from Proteintech (Rosemont, IL, USA). Anti-ATGL (2138, RRID: AB_2167955), anti-HSL (4107, RRID:AB_2296900), anti-phospho HSL (Ser660) (4126, RRID:AB_490997), anti-phospho HSL (Ser563) (4139, RRID:AB_2135495) and anti-GAPDH antibodies (2118L, RRID: AB_561053) were purchased from Cell Signaling (Danvers, MA, USA). Anti-Lamin B1 (ab16048, RRID:AB_443298) was purchased from Abcam (Cambridge, MA, USA). Anti-α-tubulin (T6074, RRID:AB_477582), anti-β-actin (A3854, RRID:AB_262011) and peroxidase-conjugated goat anti-mouse IgG (A4416, RRID:AB_258167) were purchased from Sigma-Aldrich (St. Louis, MO, USA), and peroxidase-conjugated goat anti-rabbit IgG (ZB2301, RRID:AB_2747412) was purchased from Zhongshan Golden Bridge Biotechnology (Beijing, China).

2.2. Human plasma samples

Plasma was obtained from 58 individuals with hyperhomocysteinemia and 52 nonhyperhomocysteinemia from Peking University Third Hospital and was approved by the Ethics Committee of Peking University Third Hospital. Informed consent prior to participation was provided by all subjects. The demographic data are listed in Table S1.

2.3. Animals and treatments

Male C57BL/6 mice (8 weeks old) or *Hif1a*$^{\Delta Adipo}$ mice (8 weeks old) were fed a standard diet or a high-methionine (2% L-methionine) diet (HFK Biosciences, Beijing, China) for 8 weeks to establish the HHcy model. HHcy model was also implemented by administration with Hcy (1.8 g/L) in drinking water for 2 and 4 weeks. The deletion of adipocyte HIF1α (*Hif1a*$^{\Delta adipo}$) and adipocyte-specific *Hif1a* transgenic (Ad*Hif1a*$^{LSL/LSL}$) were generated using the Cre-loxP system. The *Hif1a* flox (H*if1a*$^{f/f}$, RRID: MGI_3815313) and *Hif1a*$^{LSL/LSL}$ mice were described in an earlier study [25–27]. All animal studies were performed in compliance with the guidelines of the Institute of Laboratory Animal Resources and were approved by the Animal Care and Use Committee of Peking University.

2.4. Cell culture

Frozen 3T3-L1 cells, a mouse fibroblast-like preadipocyte line (Cat. 3111C0001CCC000155), were purchased from the Cell Resource Center of China (Beijing, China). 3T3-L1 cells were thawed and then incubated (37 °C, 5% CO_2) in Dulbecco's modified Eagle's medium (DMEM) containing 10% fetal bovine serum (FBS) (Gibco, Grand Island, NY) until confluency. Confluent 3T3-L1 cells were then incubated in differentiation medium containing 1.5 μM insulin, 1 μM dexamethasone, and 0.5 mM isobutyl methylxanthine (Sigma, St. Louis, MO) for 2 days. The cells were then transferred to DMEM with 10% FBS for an additional 4 days until they had fully differentiated into mature adipocytes. The differentiated 3T3-L1 cells were treated with reagents after being incubated in DMEM with 1% FBS for 2 h.

2.5. Body composition

An Echo 3-in-1 nuclear magnetic resonance (NMR) analyzer (Echo Medical Systems, Houston, TX) was used to measure body composition in nonanesthetized mice.

2.6. Plasma metabolites measurement

Gas chromatography-mass spectrometry was used to quantify total

Hcy and Methionine (Met) levels in plasma. The HHcy animal model had a plasma Hcy level of 19.48 ± 0.79 μM, compared with 5.76 ± 0.11 μM (Fig. S1A) in control mice. S-Adenosylmethionine (SAM) and S-Adenosyl-L-homocysteine (SAH) were examined by ELISA kit (Dogesce, Beijing, China).

2.7. Lipolysis assay

For the *in vitro* lipolysis assay, 15 mg of adipose tissue was collected and cultured in 100 μl of lipolysis buffer (Krebs buffer plus 0.1% glucose and 3.5% fatty-acid-free BSA) in a 96-well plate for 2 h at 37 °C, and then glycerol or FFAs were measured. 1-h glycerol release was examined for the indicated time in freshly changed medium. Plasma FFAs and glycerol were measured in mice after 24 h of fasting. FFAs were quantified by a NEFA assay (Wako Diagnostics, Japan), and glycerol was quantified by an enzyme-coupled colorimetric assay (GPO Trinder reaction) with a colorimetric assay kit (Applygen Technologies, Beijing, China).

2.8. Clinical biochemical measurements

Total triglyceride (TG) and cholesterol (TC) in the liver, eWAT and plasma were measured (TGKIT and TCKIT, BioSino Bio-Technology and Science, Beijing, China) to evaluate dyslipidemia and hepatic steatosis.

2.9. ChIP assay

Briefly, 3T3-L1 adipocytes were treated with 500 μM Hcy for 24 h, and the chromatin was cross-linked in 1% formaldehyde, followed by quenching with glycine for 5 min. Cross-linked chromatin nuclear extracts were fragmented, and the nuclear lysate was purified by centrifugation. Soluble chromatin was incubated with anti-HIF1α. Sepharose beads were added to chromatin and incubated overnight. The ChIP reactions were washed with wash buffer, and chromatin was eluted with elution buffer. Samples were purified with DNA purification spin columns. Genes were quantitated by quantitative PCR (qPCR) and resolution of the PCR bands on gels.

2.10. Histological analysis

Liver tissues were fixed in 4% paraformaldehyde for 6 h and dehydrated in a 20% sucrose solution overnight, and then liver tissue was embedded with OCT. Frozen liver sections were stained with Oil Red O for 30 min, and the nuclei were counterstained with hematoxylin for 30 s followed by microscopic examination.

2.11. Luciferase reporter assay

The *Ero1a* promoter was cloned into the KpnI and XhoI sites of pGL3-basic luciferase reporter vector (Promega, WI, USA). Recombinant *Ero1a* promoter reporter vectors, phRL-TK Renilla luciferase control vector and murine HIF1α triple mutants expression plasmid [28] or corresponding empty vector were transfected into 293T cells for 24 h. The luciferase assays were performed with a dual-luciferase assay system (Promega, Madison, WI, USA, E1910).

2.12. Recombinant lentivirus construction

The cDNA of HA-labeled ERO1α, FLAG-luciferase and GFP were subcloned into the pLE4 lentiviral vector provided by Dr. G.H. Liu (Institute of Biophysics, Beijing, China). The shRNA sequence targeting *Ero1a* (CAGCTCTTCACTGGGAATAAA) was cloned into pLVTHM/GFP (Addgene, Beijing, China, B12247), as described in an earlier study [24]. Recombinant lentiviral vectors were cotransfected with packaging plasmids psPAX2 (Addgene) and pMD2G (Addgene) to generate lentiviral particles from 293T cells.

2.13. Determination of intracellular H_2O_2

Intracellular H_2O_2 was determined using an Amplex red hydrogen peroxide/peroxidase assay kit (Invitrogen, Carlsbad, CA, USA, A22188).

2.14. Immunostaining

The cells were fixed with 4% paraformaldehyde for 20 min, permeabilized with 0.1% Triton for 20 min, blocked for 1 h, and then incubated with primary antibody (1:50 dilution) overnight at 4 °C and with secondary antibody (1:500 dilution) at room temperature for 1 h. LDs were stained with LipidTOX (1: 200 dilution) for 20 min.

2.15. Western blot analysis

The adipose tissue or 3T3-L1 cells were lysed in RIPA lysis buffer with protease inhibitor. Equal amounts of protein were separated by SDS-PAGE on a 10% running gel and then electrotransferred to a polyvinylidene fluoride membrane. After being blocked with 10% bovine serum albumin, the membrane was successively incubated with different antibodies (1:1000) overnight at 4 °C and then incubated with secondary antibody for 1 h at room temperature. The immunofluorescence intensities of bands were detected by the Odyssey infrared imaging system (LI-COR Biosciences, Lincoln, NE, USA). Quantitative analysis was performed using ImageJ software.

2.16. qPCR analysis

Two micrograms of RNA prepared using TRIzol reagent (Promega, Madison, WI, USA) was reverse transcribed into cDNA using a reverse transcription system (Promega, Madison, WI, USA). qPCR was carried out using SYBR Green I fluorescence and a Mx3000 Multiplex Quantitative PCR System (Agilent, La Jolla, CA, USA). All results were calculated using Stratagene Mx3000 software, and the relative mRNA levels were normalized to β-actin.

2.17. Statistical analysis

The data were analyzed using GraphPad Prism 7.0 software (GraphPad Software, San Diego, CA, USA) and IBM SPSS 24.0 (IBM Corporation, Armonk, NY). All results are presented as the means ± SEM. Shapiro-Wilk normality test is used to determine whether the data is the normal distribution. For normal distribution comparisons, student t-test or one-way ANOVA with Tukey's or Dunnett's T3 post hoc analysis were performed. Mann-Whitney *U* test (between two groups) or Kruskal-Wallis test (between multiple groups) were used to compare non-normal distributed data. $P < 0.05$ was considered statistically significant.

3. Results

3.1. Hcy activates the lipolytic process in adipose tissue

Fasting plasma Hcy and TG levels were assessed in 58 individuals with HHcy (defined as plasma Hcy > 15 μM) and 52 controls. Total subjects were 45.4 ± 1.5 years old and had a BMI at 22.1 ± 0.2 (Table S1). We found that plasma TG concentrations were positively correlated with Hcy levels (Fig. 1A) and that plasma FFAs also had a positive correlation with Hcy (Fig. 1B). To investigate the effect of Hcy on lipid changes in plasma, we fed C57BL/6 mice a normal chow diet or a high-methionine diet (HMD) for 8 weeks, which is regarded as a commonly used HHcy model [29,30]. The plasma levels of Hcy were markedly increased after HMD treatment and related metabolites concentrations (SAM and SAH) in the methionine cycle were also raised, which established HHcy mice. While an increasing trend was observed for methionine, this was consistent with the result previously reported by others [31] (Figs. S1A–S1D). The body weight of HHcy mice was

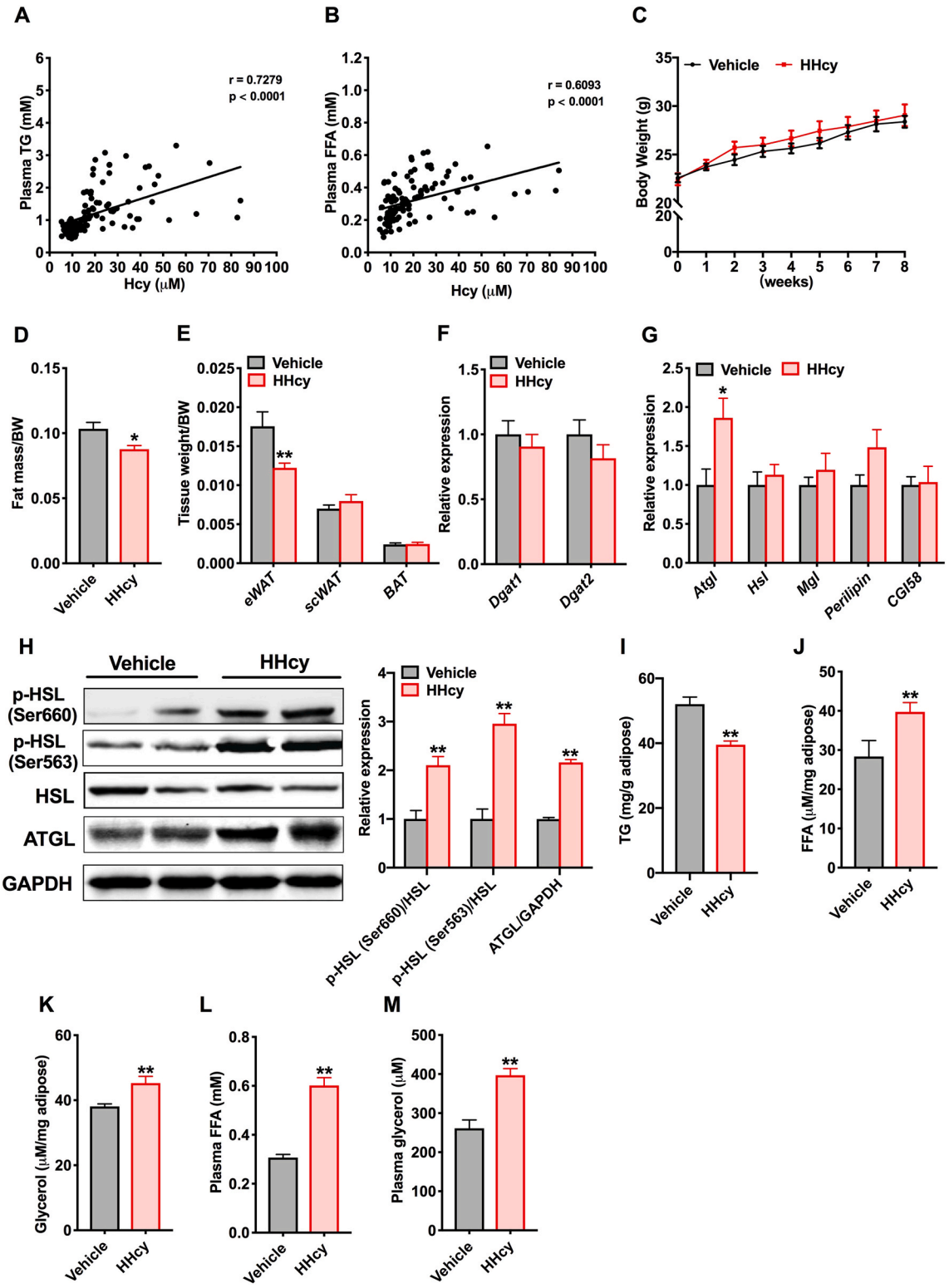

Fig. 1. Hcy elevates the lipolytic process in adipose tissue

(A, B) Correlation analysis of plasma Hcy levels with TG or FFAs levels in human samples (n=110 total individuals)

C57BL/6 mice (8 weeks old) were maintained on a normal chow diet (NCD, vehicle) or a 2% L-methionine diet (high-methionine diet, HMD) for 8 weeks. (C) Weekly changes in body weight (n=6). (D) At the eighth week, the fat mass ratio was measured by NMR (n=6). (E) Ratios of epididymal white adipose tissue (eWAT), subcutaneous white adipose tissue (scWAT) and brown adipose tissue (BAT) weight to body weight (BW) (n=6). (F) qPCR analysis of the mRNA levels of *Dgat1* and *Dgat2* in eWAT (n = 6). (G) The relative expression of genes involved in adipose tissue lipolysis (n = 6). (H) Protein levels of ATGL and phosphorylation levels of HSL at the Ser660 and Ser563 residues (n = 3). (I) TG content in the eWAT (n = 6). (J, K) FFAs and glycerol released from the eWAT of vehicle and HHcy mice that were fasted for 24 h (n = 6). (L, M) Plasma FFAs and glycerol levels in vehicle and HHcy mice (n = 6). All of the data are presented as the means ± SEM. (A, B) Pearson's correlation: $P < 0.01$ for TG; $P < 0.01$ for FFA. (C, D, F-M) Two-tailed Student's t-test and (E) Mann-Whitney *U* test: $^{*}P < 0.05$, $^{**}P < 0.01$ compared to the vehicle group. . (For interpretation of the references to color in this figure legend, the reader is referred to the Web version of this article.)

similar to that of the vehicle mice, but Hcy treatment resulted in less fat mass than vehicle treatment (Fig. 1C and D). Consistent with this result, the HHcy mice displayed decreased epididymal white adipose tissue (eWAT) weight, but the subcutaneous adipose tissue (scWAT) and brown adipose tissue (BAT) were not affected (Fig. 1E). Next, we supposed that the lower eWAT weight observed in HHcy mice was the result of decreased lipid synthesis or enhanced lipolysis. The mRNA expression of genes involved in TG synthesis (*Dgat1* and *Dgat2)* and adipocyte lipolysis (*Atgl*, *Hsl*, *Mgl*, *Perilipin* and *CGI-58*) was detected. Hcy had no effect on the process of TG synthesis but increased the mRNA levels of the gene *Atgl* (adipose triglyceride lipase) (Fig. 1F and G). Simultaneously, Hcy upregulated ATGL protein levels and promoted HSL (hormone-sensitive lipase) phosphorylation at the Ser660 and Ser563 residues, two critical phosphoserine sites for regulating HSL activity (Fig. 1H). ATGL and HSL are two vital enzymes in the process of lipolysis that together regulate hydrolysis of TG into FFAs and glycerol in adipose tissue [32]. Furthermore, TG content in eWAT was decreased, and the levels of FFAs and glycerol were increased in eWAT of the HHcy mice compared to the vehicle mice, and both were also raised in plasma (Fig. 1I–M). Similarly, we also found activation of lipase in the mice administered Hcy in the drinking water and increased levels of FFAs and glycerol in plasma as early as 2 weeks (Figs. S1E–S1H). In order to evaluate the lipolysis action *in vitro*, isolated mice eWAT was treated with Hcy. As shown in Fig. S1I, the glycerol release per hour in the medium was increased in the Hcy group compared to control. And Hcy-induced increased glycerol release was partially abrogated after administration of lipolysis inhibitors (Figs. S1J and S1K). Above all, enhanced levels of FFAs and glycerol, together with increased lipase activity in the HHcy mice, indicate that Hcy induces the adipocyte lipolytic response.

3.2. Hcy aggravates ectopic deposition of lipids in the liver

Adipose tissue stores energy in the form of TG and hydrolyzes it into FFAs for other organs. In various organs, hepatic FFAs are mostly derived from adipose tissue (60%) [33]. In the HHcy mice, the expression of fatty acid (FA) metabolic genes in the liver revealed the upregulation of *Cd36*, a gene associated with FA uptake, but the expression of the lipogenesis genes and FA β-oxidation genes remained unchanged compared with the vehicle mice (Fig. 2A). Furthermore, Oil Red O staining showed that hepatic LD accumulation was elevated in the HHcy mice (Fig. 2B). HHcy mice also displayed substantially higher liver weight compared to that of controls (Fig. 2C). In addition, hepatic TG and plasma TG levels were also increased, while there was no significant differences in hepatic total cholesterol (TC) and plasma TC levels compared with the vehicle mice (Fig. 2D–G). Thus, these results indicate that Hcy leads to perturbed lipid uptake in the liver.

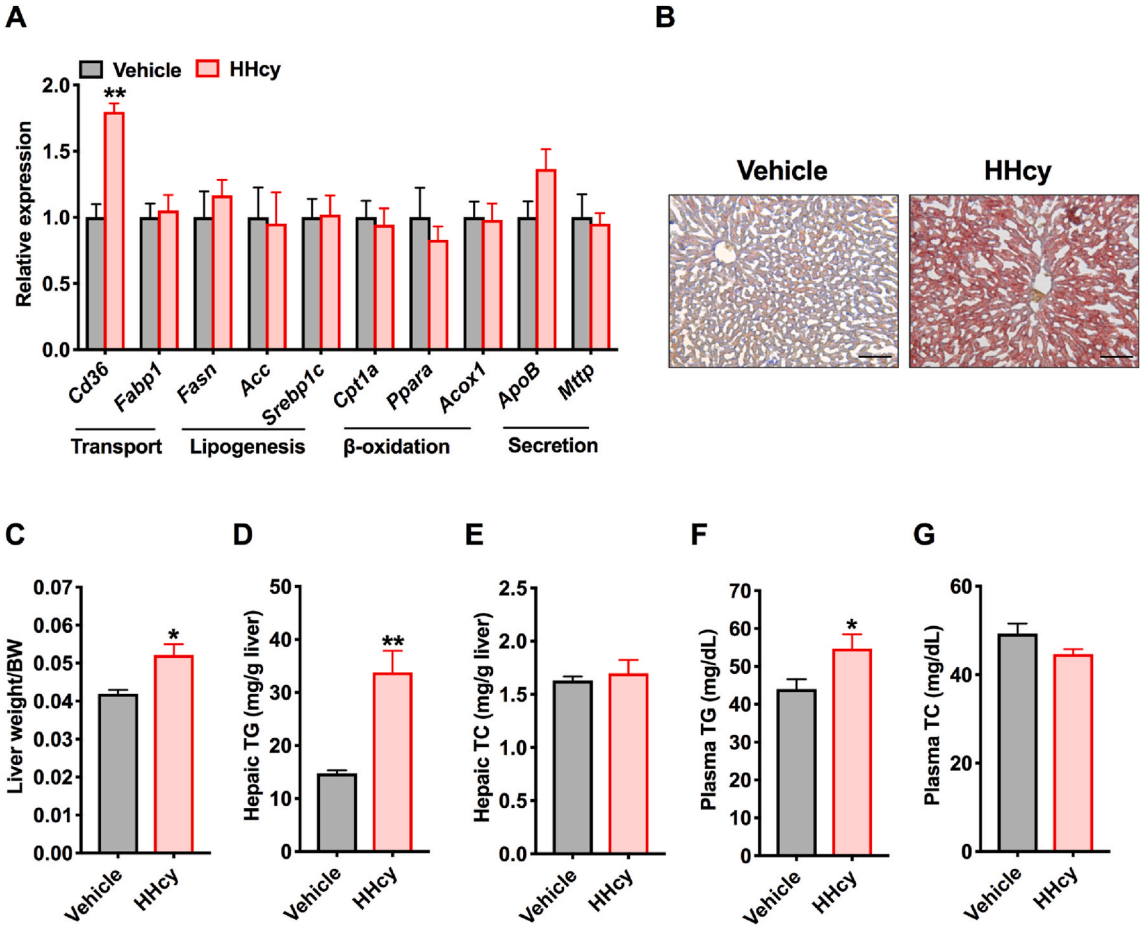

Fig. 2. Hcy aggravates ectopic deposition of lipids in the liver

C57BL/6 mice (8 weeks old) were maintained on an NCD or an HMD for 8 weeks

(A) The relative expression of genes involved in fatty acid transport, fatty acid anabolism, β-oxidation and TG secretion (n = 6). (B) Representative Oil Red O staining of lipids in liver sections. Scale bars, 100 μm (n = 6). (C) Ratio of liver weight to body weight (n = 6). (D, E) TG and TC contents of the liver (n = 6). (F, G) Plasma TG and TC levels (n = 6). All of the data are presented as the means ± SEM. (A, C-G) Two-tailed Student's t-test: $^{*}P < 0.05$, $^{**}P < 0.01$ compared to the vehicle group. . (For interpretation of the references to color in this figure legend, the reader is referred to the Web version of this article.)

3.3. Inhibition of lipolysis decreases Hcy-induced NAFL

To study whether Hcy-induced liver lipid accumulation is due to lipolysis of adipose tissue. HHcy mice were treated with acipimox, a potent chemical inhibitor of lipolysis. Treatment with acipimox (0.08 g kg^{-1} day^{-1}) alone for 8 weeks had no effects on body weight but blunted the decrease in eWAT weight (Fig. 3A and B). In addition, administration of acipimox alleviated the release of plasma FFAs and glycerol (Fig. 3C and D), as well as the levels of FFAs and glycerol in eWAT in HHcy mice (Fig. 3E and F). Furthermore, Oil Red O staining showed that hepatic lipid accumulation was decreased after acipimox intervention (Fig. 3G). Administration of acipimox to HHcy mice also prevented the Hcy-induced increase in TG concentrations and liver weight (Fig. 3H and I). These data suggest that Hcy-induced adipose tissue lipolysis is the key event linking increased hepatic TG levels with elevated release of FFAs.

3.4. Hcy promotes adipocyte lipolysis via ERO1α-dependent ER overoxidation, ER stress and ER-LD interaction

In our previous work, we found that Hcy activates adipocyte ER stress, which is involved in insulin resistance [9]. Moreover, it has been reported that the occurrence of ER stress augments lipolysis *in vivo* and subsequently leads to fatty infiltration of the liver [14,34]. Next, we verified whether ER stress is responsible for the Hcy-induced lipolysis

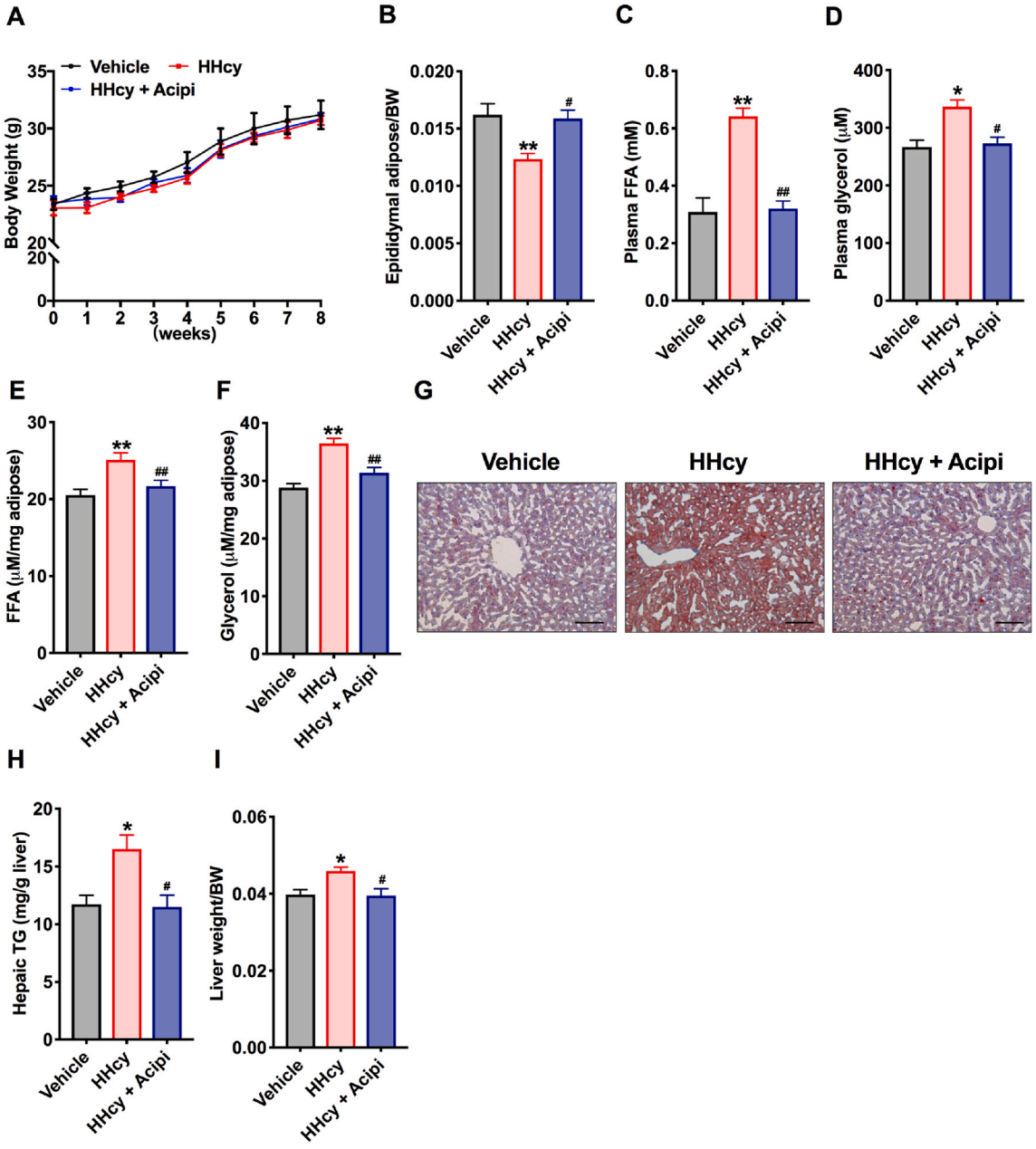

Fig. 3. Inhibition of lipolysis improves Hcy-induced NAFL
C57BL/6 mice (8 weeks old) were treated with Veh, HMD or HMD + acipimox. (A) Body weight changes (n=5). Acipi, acipimox. (B) Ratio of eWAT weight to BW (n=5). (C, D) Plasma FFAs and glycerol levels after fasting for 24
h (n=5). (E, F) FFAs and glycerol levels released from eWAT (n=5). (G) Representative Oil Red O staining of lipids in liver sections. Scale bars, 100 μm (n=5). (H) Hepatic TG levels (n=5). (I) Ratio of liver weight to BW (n=5). All of the data are presented as the means ± SEM. (A-C, E, F, H, I) One-way ANOVA with Tukey's post-hoc test and (D) Kruskal-Wallis test: $^{*}P < 0.05$, $^{**}P < 0.01$ compared to the vehicle group. $^{\#}P < 0.05$, $^{\#\#}P < 0.01$ compared to the HHcy group. . (For interpretation of the references to color in this figure legend, the reader is referred to the Web version of this article.)

process. ER stress markers were detected, including *Atf6*, *Atf4*, *Chop*, ER chaperones (*Bip*) and an ER oxidoreductase (*Ero1α)* [35]. The levels of *Atf4*, *Chop*, *Bip* and *Ero1a* were evaluated in the eWAT of HHcy mice; interestingly, *Ero1a* was the most obvious (Fig. S2A). Simultaneously, the protein levels of ERO1α were upregulated in the adipose tissue of HHcy mice (Fig. 4A and S2B). In addition, Hcy (500 μM) upregulated the expression of ERO1α in 3T3-L1 cells as early as 1 h in a time-dependent manner *in vitro* (Fig. 4B). ERO1α utilizes molecular oxygen to generate disulfide and H_2O_2, therefore, the levels of H_2O_2 were detected by using the Amplex red peroxide/peroxidase assay. As we expected, Hcy time-dependently increased H_2O_2 production in 3T3-L1 cells (Fig. 4C).

To further examine whether ERO1α mediated the Hcy-induced lipolytic process, we used lentiviral shRNA vectors to knock down ERO1α in 3T3-L1 cells. As shown in Figs. S2C and S2D, Hcy-induced upregulation of ERO1α protein and mRNA levels was markedly inhibited after using lentiviral shRNA vectors. Specifically, the accumulation of H_2O_2 and upregulation of ER stress markers (*Atf4*, *Chop*, and *Bip*) by Hcy treatment were also attenuated (Fig. 4D and E). In addition, small GTPase Rab18 localization was increased on LDs under Hcy treatment but was decreased after knockout of ERO1α (Fig. 4F). Rab18 is shown to co-localize the ER-LD surface and plays an important role in ER-LD contacts, which was also reported that mediate β-adrenergic–stimulated lipolysis [36,37]. More importantly, ERO1α deficiency reduced the release of FFAs and glycerol in the supernatant after Hcy treatment (Fig. 4G and H). The above results suggest that Hcy activates cellular oxidative stress and ER-LD interaction by upregulating the expression of ERO1α, which both contribute to Hcy-induced adipose tissue lipolysis.

3.5. Activation of HIF1α mediates ERO1α upregulation and H_2O_2 accumulation in adipocytes

Oxygen deprivation is a key factor that leads to ER oxidative stress and ER stress [21,38]. HIF1α is well known as the main mediator of the hypoxia response in adipose tissue [57,39], and our previous work has revealed that inhibition of HIF1α in adipocytes improves insulin resistance and decreases the levels of proinflammatory cytokines [40]. Indeed, Western blot analysis revealed that HIF1α was activated in HHcy mice compared with vehicle mice, but there was no difference in mRNA levels (Figs. S3A and S3B). In adipocytes, treatment with the general HIF1α inhibitor acriflavine (ACF, 5 μM) significantly attenuated Hcy-induced ERO1α expression (Fig. 5A). We then implemented adipocyte-specific disruption of the *Hif1a* gene via Cre-loxP–mediated recombination and treated control mice ($Hif1a^{f/f}$) and adipocyte-specific HIF1α ($Hif1a^{\Delta adipo}$) mice with an HMD for 8 weeks. As we expected, the expression of HIF1α mRNA was specifically decreased in adipose tissue in $Hif1a^{\Delta Adipo}$ mice compared with that in $Hif1a^{f/f}$ mice. The induction of the HIF1α target gene *Pdk1* was markedly attenuated in the adipose tissue of $Hif1a^{\Delta Adipo}$ mice, which confirmed that the loss of HIF1α was of functional significance (Fig. S3C).

In $Hif1a^{\Delta Adipo}$ mice, both the mRNA and protein levels of ERO1α were decreased (Fig. 5B and C), but ERO1α was upregulated in Ad$Hif1a^{LSL/LSL}$ mice (adipocyte-specific HIF1α overexpression) compared to that of $Hif1a^{+/+}$ mice (Fig. S3D, 5D and 5E). HIF1α binds to target genes by recognizing hypoxia regulatory elements (HREs), and we found two putative HREs within the promoter of *Ero1a* (Fig. 5F). Furthermore, ChIP analysis was performed. The results showed that *Ero1a* contained potential HRE1 but not HRE2 site, which could be directly enhanced the binding with HIF1α after Hcy stimulation (Fig. 5G). A luciferase reporter assay further showed that greater transcriptional activity of the *Ero1a* promoter exists with constitutively active HIF1α triple mutants (HIF1αTM) transfection. After double mutation of HRE or single mutation of HRE1, the increased transcription activity of *Ero1a* promoter induced by HIF1αTM was abolished, but was not affected by the HRE2 mutation, indicating that HIF1α directly binds HRE1 of the *Ero1a* promoter to mediate ERO1α expression elevation (Fig. 5H). In addition, the accumulation of H_2O_2 in 3T3-L1 cells and ER stress in adipocytes were both reduced (Fig. 5I and J). Taken together, these results show that adipocyte HIF1α mediates Hcy-induced ERO1α expression elevation and ERO1α-dependent H_2O_2 accumulation in adipocytes.

3.6. Deletion of adipocyte HIF1α ameliorates Hcy-induced adipose lipolysis and NAFL

To investigate the importance of adipocyte HIF1α in Hcy-induced lipolysis and the development of NAFL, $Hif1a^{f/f}$ and $Hif1a^{\Delta Adipo}$ mice were administered HMD for 8 weeks. Body weight was comparable in $Hif1a^{f/f}$ and $Hif1a^{\Delta Adipo}$ mice, but the Hcy-induced decreased fat mass, eWAT weight and TG content were partially abrogated in $Hif1a^{\Delta Adipo}$ mice compared to $Hif1a^{f/f}$ mice (Fig. 6A–D). The disruption of adipose HIF1α substantially reversed the release of FFAs and glycerol from eWAT, as well as the increase in plasma FFAs and glycerol (Fig. 6E–H). The lipolytic gene was downregulated in Hcy-treated $Hif1a^{\Delta Adipo}$ mice, but with no differences in TG synthesis and fatty acid oxidation genes (Figs. S4A–S4C). Taken together, these results suggest that adipocyte-selective inactivation of HIF1α weakens the Hcy-induced lipolytic process. Next, changes of lipids in the liver were examined. Oil Red O staining revealed a reduction in hepatic LDs in $Hif1a^{\Delta Adipo}$ mice (Fig. 6I). Hcy-induced increases in liver weight and hepatic TG levels were abrogated after disruption of adipose HIF1α but with no changes in hepatic TC levels (Fig. 6J–L). Furthermore, along with diminished HIF1α signaling in adipose tissue, CD36 mRNA levels were repressed in $Hif1a^{\Delta Adipo}$ mice compared with those of $Hif1a^{f/f}$ mice (Fig. 6M). These results reveal that adipocyte-specific deletion of HIF1α alleviates the Hcy-induced lipolysis process and ectopic lipid accumulation in the liver.

4. Discussion

NAFLD is now identified as the most common chronic liver disease in developed and developing countries [41]. In the last few decades, HHcy has become a risk factor for several diseases and has been considered an important health issue [42]. Previous research has also uncovered that Hcy plays a vital role in the function of adipose tissue [8,42]. Here, our study reveals that Hcy promotes the adipocyte lipolytic response and that the HIF1α-ERO1α pathway involved in ER overoxidation and ER stress is a novel mechanism of Hcy-induced lipolysis (Fig. 6N).

A hallmark of NAFL development is the accumulation of TG in hepatocytes. Hepatic lipid content is regulated by balancing four pathways involved hepatic lipid uptake, synthesis, oxidation, and export. Hepatic *de novo* lipogenesis accounts for 25% and is regulated by key transcription factors such as SREBP-1c. Notably, 60% of hepatic TG is derived from WAT lipolysis. And the other two pathways, including impaired fatty acid oxidation and impaired secretion of very low density lipoprotein, seem less important [43,44]. Here, we have found no differences in lipogenesis (*Fasn, Acc, Srebp1c*), FA β-oxidation (*Cpt1a, Ppara, Acox1*) and lipid secretion (*ApoB, Mttp*) pathways in the liver of HHcy mice. However, the upregulation of hepatic *Cd36* and the increase of FFAs in plasma and adipose, as well as the elevation of lipase indicate that adipose tissue lipolysis is the main pathway in Hcy-induced NAFL. Adipose tissue communicates with other tissues and organs to integrate systemic lipid homeostasis by controlling circulating FFAs levels. Under physiological conditions, lipid storage and hydrolysis are balanced and tightly controlled. However, when this balance is perturbed, causing adipose tissue disorders, leading to elevated plasma FFAs levels in the bloodstream and other tissues and thereby may result in lipotoxicity, dyslipidemia and insulin resistance [14,45,46]. An increased lipolytic response may be consistent with decreased adipose tissue mass. In line with this, the eWAT weight is lower and the liver weight is higher in HHcy mice than those in controls, which accounts for why the body weight is not altered. Hcy-induced NAFL dependent on adipose lipolysis is also demonstrated by using acipimox. The antilipolytic mechanism of acipimox is through inhibition of intracellular cyclic AMP, followed by

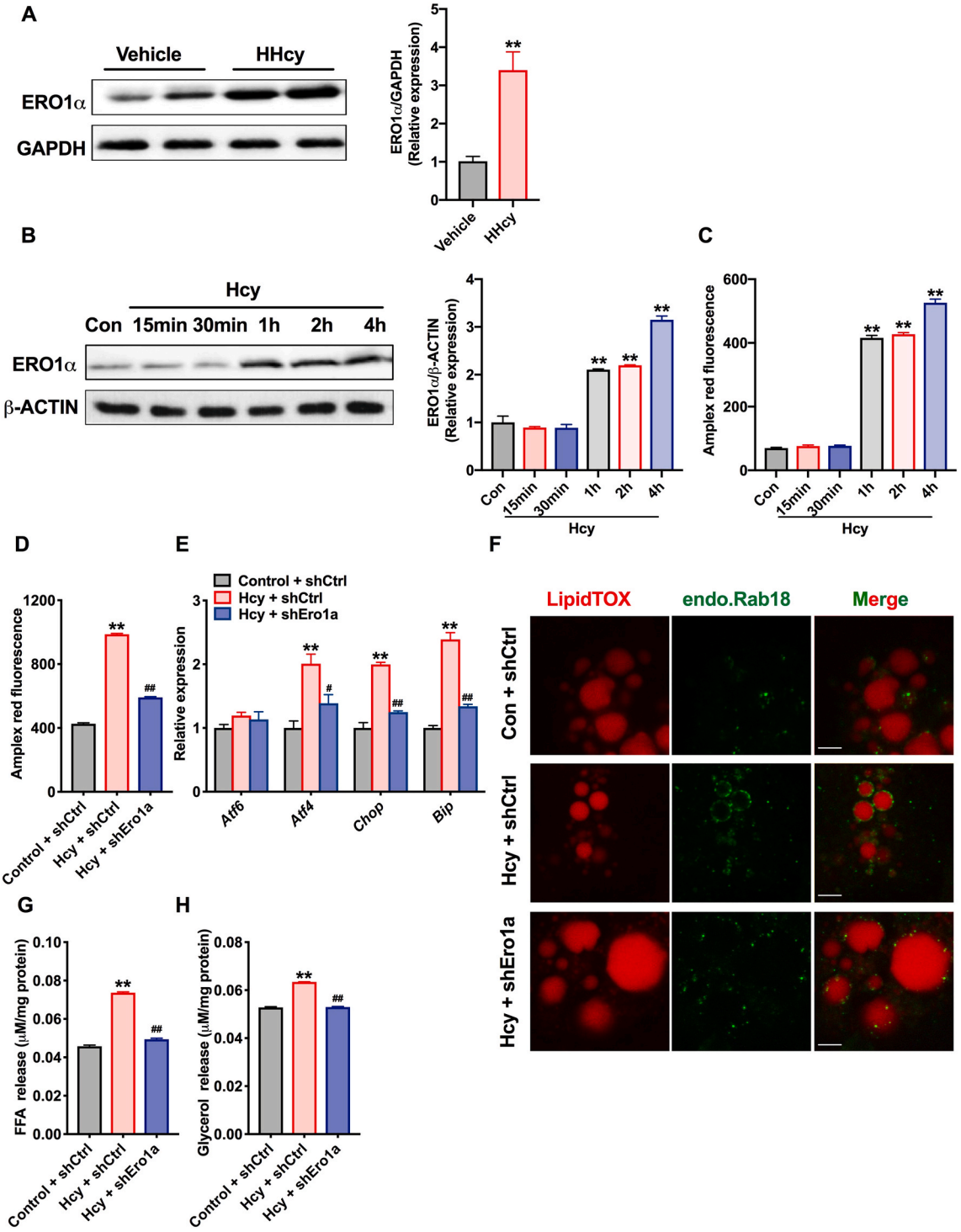

Fig. 4. Hcy promotes adipocyte lipolysis through ERO1α-dependent ER overoxidation, ER stress and ER-LD interaction

(A) Protein levels of eWAT ERO1α in the vehicle or HHcy mice (n = 3). (B) Protein levels of ERO1α in differentiated 3T3-L1 cells. The 3T3-L1 cells were treated with control or Hcy (500 μM) for the indicated lengths of time (n = 3). (C) H_2O_2 levels in 3T3-L1 cells with 500 μM Hcy for the indicated lengths of time (n = 3). 3T3-L1 cells transduced with lentiviral control shRNA (shCtrl) or shEro1a for more than 72
h were treated with 500 μM Hcy. (D, E) Intracellular H_2O_2 levels and the relative expression of genes related to ER stress markers (n = 5). (F) Location of Rab18 (green) on LDs (red) in 3T3-L1 cells. Scale bars, 3 μm (n = 3). (G, H) FFAs and glycerol in the supernatant (n = 5). All of the data are presented as the means ± SEM. (A) Two-tailed Student's t-test: $^{**}P < 0.01$ compared to the vehicle group. (B, C) One-way ANOVA with Tukey's post-hoc test: $^{**}P < 0.01$ compared to the control group. (D, E, G, H) One-way ANOVA with Tukey's post-hoc test: $^{**}P < 0.01$ compared to the control + shCtrl group. $^{\#}P < 0.05$, $^{\#\#}P < 0.01$ compared to the Hcy + shCtrl group. . (For interpretation of the references to color in this figure legend, the reader is referred to the Web version of this article.)

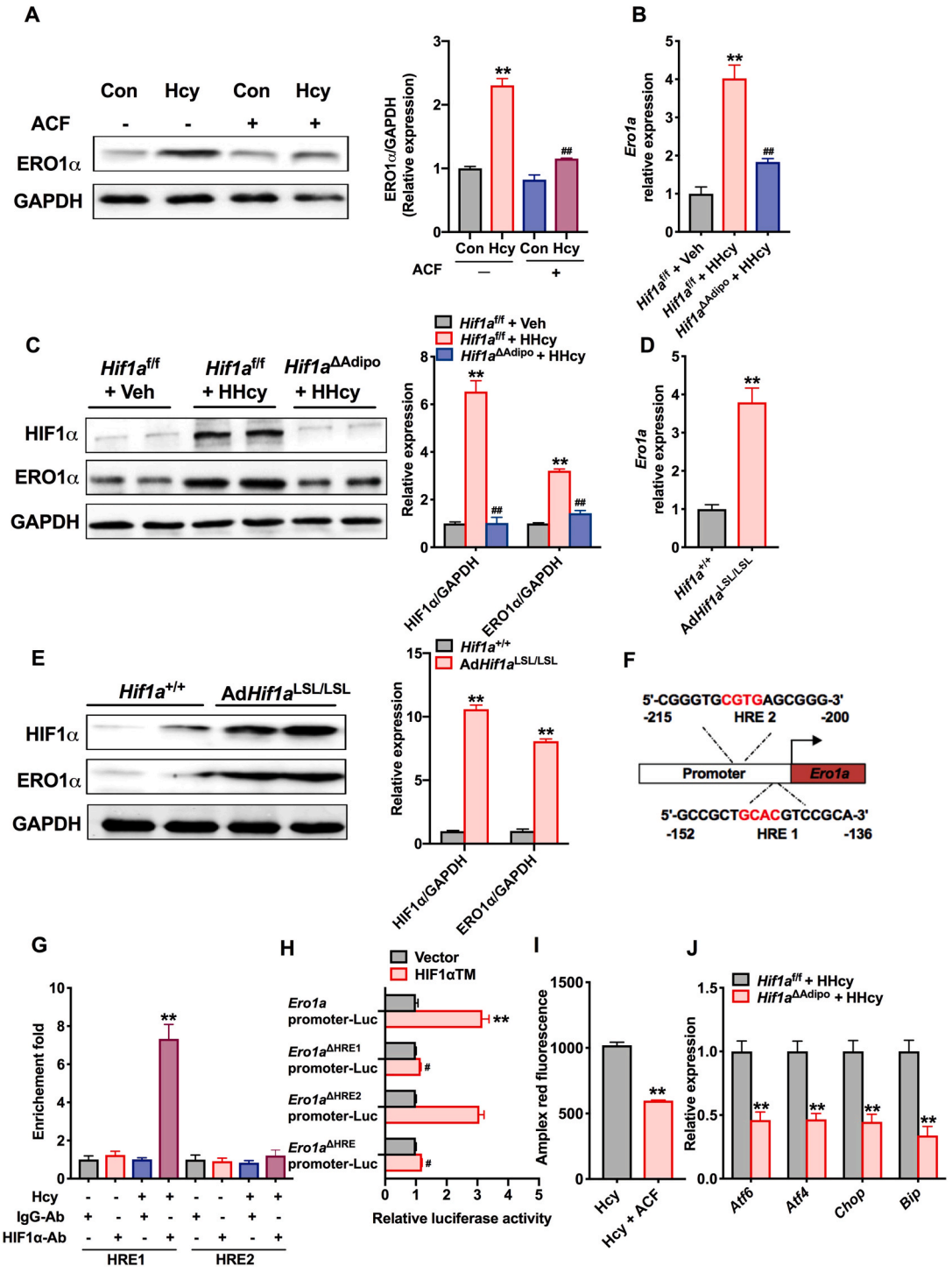

Fig. 5. Activation of HIF1α mediates Hcy-enhanced ERO1α expression in adipocytes

(A) Protein levels of ERO1α in differentiated 3T3-L1 cells. After pretreatment with ACF (5 μM) for 6 h, the 3T3-L1 cells were treated with Hcy (500 μM) for 24 h. ACF (acriflavine), HIF1α inhibitor (n = 3). One-way ANOVA with Tukey's post-hoc test: $^{**}P < 0.01$ compared to the control group. $^{\#\#}P < 0.01$ compared to the Hcy group.

Hif1a$^{f/f}$ or *Hif1a*$^{\Delta Adipo}$ mice (8 weeks old) were maintained on an NCD or an HMD for 8 weeks. (B) qPCR analysis of the mRNA levels of *Ero1a* (n = 6). (C) Protein levels of ERO1α and HIF1α in the eWAT of *Hif1a*$^{f/f}$ and *Hif1a*$^{\Delta Adipo}$ mice after 8 weeks on an NCD or an HMD (n = 4). (B, C) One-way ANOVA with Tukey's post-hoc test: $^{**}P < 0.01$ compared to the *Hif1a*$^{f/f}$ + Veh group. $^{\#\#}P < 0.01$ compared to the *Hif1a*$^{f/f}$ + HHcy group. (D, E) mRNA and protein levels of ERO1α in the eWAT of *Hif1a*$^{+/+}$ and Ad*Hif1a*$^{LSL/LSL}$ mice (n = 6 or 4). Two-tailed Student's t-test: $^{**}P < 0.01$ compared to the *Hif1a*$^{+/+}$ group. (F) Schematic diagram of the HREs in the murine *Ero1a* gene. (G) ChIP assays in 3T3-L1 cells (n = 6). One-way ANOVA with Tukey's post-hoc test: $^{**}P < 0.01$ compared to the IgG-Ab group. (H) Luciferase assay of *Ero1a* transcription activity (n = 6). HIF1αTM, overexpression of a constitutively active HIF1α triple mutants plasmid. One-way ANOVA with Tukey's post-hoc test: $^{**}P < 0.01$ compared to the *Ero1a* promoter plasmid with vector group. $^{\#\#}P < 0.01$ compared to the *Ero1a* promoter plasmid with HIF1αTM group. (I) H_2O_2 levels in 3T3-L1 cells treated with or without ACF (5 μM) for 6 h and Hcy (500 μM) for 24 h (n = 6). Two-tailed Student's t-test: $^{**}P < 0.01$ compared to the Hcy group. (J) The relative expression of genes related to ER stress markers in *Hif1a*$^{f/f}$ and *Hif1a*$^{\Delta Adipo}$ mice (n = 6). Two-tailed Student's t-test: $^{**}P < 0.01$ compared to the *Hif1a*$^{f/f}$ + HHcy group. All of the data are presented as the means ± SEM.

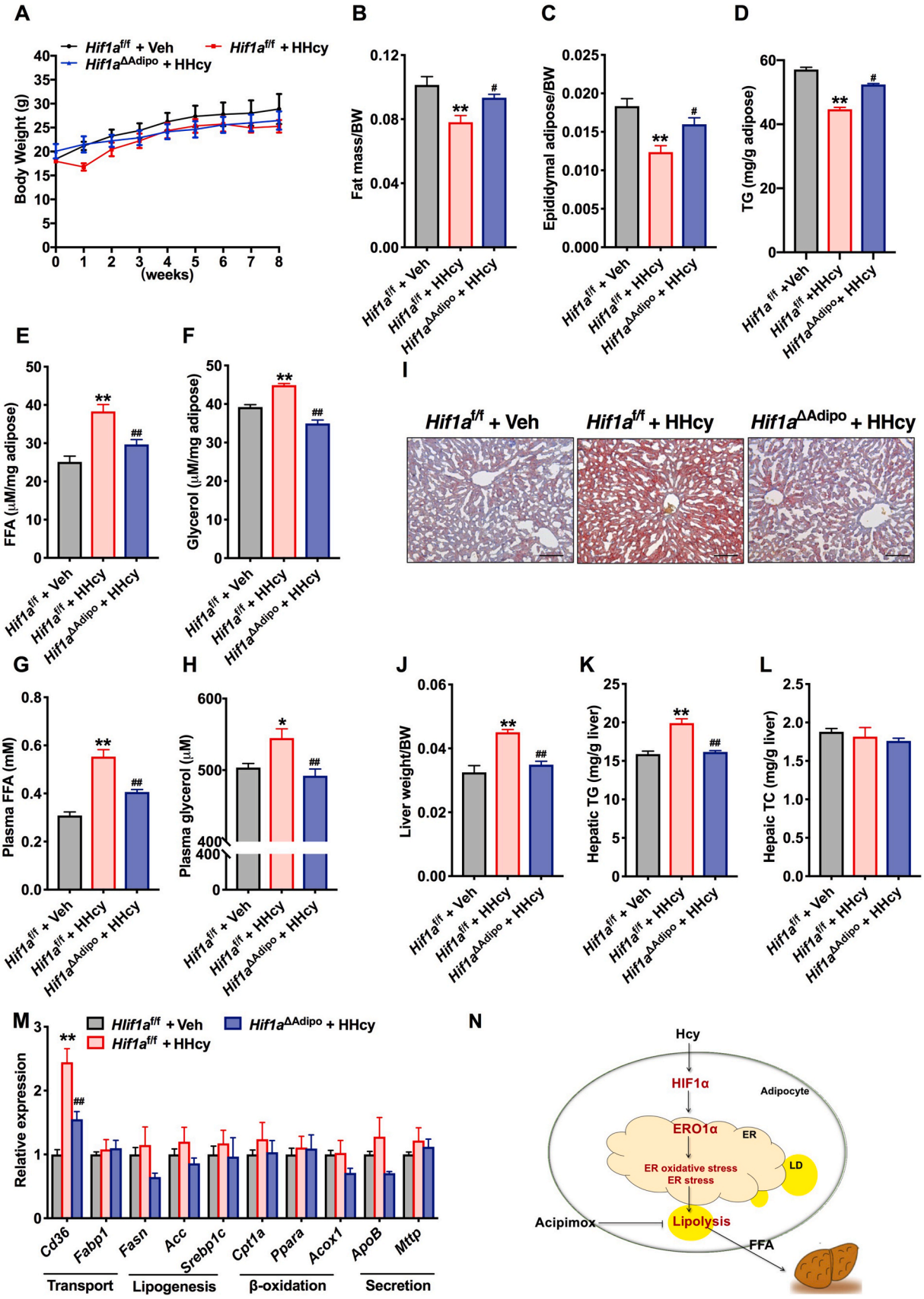

(caption on next page)

Fig. 6. Adipocyte specific HIF1α ablation alleviates Hcy-enhanced lipolysis and NAFL
Hif1a$^{f/f}$ or *Hif1a*$^{\Delta Adipo}$ mice (8 weeks old) were maintained on an NCD or an HMD for 8 weeks. (A) Weekly changes in body weight (n = 5). (B) At the eighth week, the fat mass ratio was measured by NMR (n = 5). (C) Ratio of eWAT weight to body weight (n = 5). (D) TG content in eWAT (n = 5). (E, F) The levels of FFAs and glycerol released from eWAT (n = 5). (G, H) Plasma FFAs and glycerol concentrations (n = 5). (I) Representative Oil Red O staining of lipids in liver sections. Scale bars, 100 μm (n = 5). (J) Ratio of liver weight to body weight (n = 5). (K, L) TG and TC contents in the liver (n = 5). (M) The relative expression of genes involved in fatty acid transport, fatty acid anabolism, β-oxidation and TG secretion (n = 5). (N) A schematic diagram summarizing the findings that Hcy promotes the HIF1α-ERO1α pathway involved in ER overoxidation stress and ER stress that contributes to NAFL progression. All of the data are presented as the means ± SEM. (A) Kruskal-Wallis test, (B–H, M) One-way ANOVA with Tukey's post-hoc test and (J–L) One-way ANOVA with Dunnett's T3 post-hoc test: $^{*}P < 0.05$, $^{**}P < 0.01$ compared to the *Hif1a*$^{f/f}$ + Veh group. $^{\#}P < 0.05$, $^{\#\#}P < 0.01$ compared to the *Hif1a*$^{f/f}$ + HHcy group. . (For interpretation of the references to color in this figure legend, the reader is referred to the Web version of this article.)

decreased activity of cyclic AMP-dependent protein kinases, resulting in a reduced ability of HSL to hydrolyze lipids in adipocytes [47]. Acipimox is widely used to treat hypertriglyceridemia, which also improves glucose tolerance in HFD- and nicotine-treated mice, primarily by reducing FFAs levels and improving insulin sensitivity [48,49].

In our previous study, we have found that Hcy induces the occurrence of ER stress [9]. Indeed, the ER is more oxidized than other cellular components and is more sensitive to reductive stress, and it is also the main site for disulfide bond formation of secretory proteins in the cell [50,51]. In this process, ERO1α, as a sulfhydryl oxidase, generates disulfides in the lumen of the ER by transferring electrons to molecular oxygen [52]. Recent studies have showed that activation of ERO1α can generate reactive oxygen species (ROS) hydrogen peroxide and enhance IRE1 and PERK signaling caused by oxidation of UPR sensors [53], which is the link between ER overoxidation and ER stress. Interfering with the expression of ERO1α in human umbilical vein endothelial cells also inhibits activation of the IRE1 and PERK pathways [24]. In the present work, the expression of ERO1α is upregulated in the adipose tissue of HHcy mice, which contributes to the accumulation of H_2O_2, ER overoxidation and stress, further causing lipolytic response. Consistent with the studies have showed that potential consequence of prolonged ER stress within adipose tissue is chronic lipolysis, which induces FFA efflux from adipocytes to the plasma and regulates the routing of lipids to other organs for storage [34,54]. Simultaneously, in 3T3-L1 cells, we have found that Hcy treatment has resulted in Rab18 recruitment to the surface of LDs but that Rab18 recruitment decreased after interfering with ER-specific ERO1α. Rab18 has been reported to play a direct role in contacting ER and LDs, and Rab18 overexpression increases the number of ER-LD contacts [55]. Rab18 is also shown to be a common mediator in β-adrenergic-induced lipolysis and insulin-mediated lipogenesis, and ER is the link that allows Rab18 to regulate these two processes [36]. Changes in ER stress and ER homeostasis are involved in the regulation of LD lipolysis, but the interplay between them requires further study.

HIF1α is a nuclear transcription factor and functions as an oxygen-sensitive α subunit and β heterodimer (ARNT) that is stable under hypoxia [23]. In the obese mice, we have found that activation of adipose HIF1α promotes adiposity, whereas the underlying mechanism is still not clear. On the one hand, HIF1α may regulate the reduced insulin signal to promote TG store. On the other hand, it may be due to the decrease of energy expenditure and fatty acid oxidation. Indeed, the process of lipolysis has been also inhibited in HFD-treated *Hif1a*$^{\Delta Adipo}$ mice [23]. However, in HHcy mice, activation of HIF1α just mediate the process of adipocyte lipolysis, with no effect of other lipid metabolic pathways. Different models and metabolic states may account for the differences in the lipid metabolism pathway that HIF1α primarily regulates. In addition, our previous study has showed that deletion of adipocyte HIF1α ameliorates Hcy-induced insulin resistance [40]. In the present study, *Hif1a*$^{\Delta Adipo}$ mice have reduced lipolysis, which is consistent with studies showing higher lipolysis is a contributor to insulin resistance [12]. Mechanistically, *Ero1a* has been identified as a target gene of HIF1α, which yields a novel mechanism for Hcy-induced adipose lipolysis. In line with our observations, some studies have shown that oxygen provides oxidative potential for oxidative proteins and mediates the correct formation of disulfide bonds. Under oxygen deprivation, the unfolded protein accumulates in the ER and hypoxia can also cause excessive production of ROS and provoke oxidation of DNA and proteins [21,56].

In conclusion, the current study has identified that Hcy activates adipocyte lipolysis. A previously unrecognized adipocyte HIF1α-ERO1α-mediated pathway involving ER overoxidation and ER stress contributes to the Hcy-induced lipolytic process. Under physiological conditions, excessive increased adipocyte lipolysis is accompanied by a high level of circulating FFAs, which leads to lipid ectopic deposition in the liver. This phenomenon implies the vital role of adipose tissue in Hcy-induced NAFL and identifies the potential strategy of targeting ER redox homeostasis for the development of NAFL.

Author contributions

Y.Y., X.W., S.-Y.Z, L.-L.S., P.W, Y.Z, G.Z, B.L., G.X. and H.L.performed the experiments and analyzed the data. L.W., X.W. and C.J. designed and supervised the research. Y.Y., X.W. and C.J. wrote the manuscript. All authors supported the final manuscript. C.J. is the guarantor of this work and, as such, had full access to all the data in the study and takes responsibility for the integrity of the data and the accuracy of the data analyses.

Declaration of competing interest

The authors declare that they have no known competing financial interests or personal relationships that could have appeared to influence the work reported in this paper.

The authors declare the following financial interests/personal relationships which may be considered as potential competing interests:

Acknowledgments

This work was supported by the National Natural Science Foundation of the People's Republic of China (No. 31872787, 91739303, 91857115, 31925021, 81921001, 31771261 and 81700010) and the Strategic Priority Research Program of Chinese Academy of Sciences (XDB37020303).

Appendix A. Supplementary data

Supplementary data to this article can be found online at https://doi.org/10.1016/j.redox.2020.101742.

References

[1] M.V. Machado, A.M. Diehl, Pathogenesis of nonalcoholic steatohepatitis, Gastroenterology 150 (8) (2016) 1769–1777.
[2] S. Wei, S. Liu, X. Su, W. Wang, F. Li, J. Deng, et al., Spontaneous development of hepatosteatosis in perilipin-1 null mice with adipose tissue dysfunction, Biochim. Biophys. Acta 1863 (2) (2018) 212–218.
[3] C.D. Fuchs, T. Claudel, M. Trauner, Role of metabolic lipases and lipolytic metabolites in the pathogenesis of NAFLD, Trends Endocrinol. Metabol. 25 (11) (2014) 576–585.
[4] M. Gulsen, Z. Yesilova, S. Bagci, A. Uygun, K. Dagalp, Elevated plasma homocysteine concentrations as a predictor of steatohepatitis in patients with non-alcoholic fatty liver disease, J. Gastroenterol. Hepatol. 20 (9) (2005) 1448–1455.
[5] P. Ganguly, S.F. Alam, Role of homocysteine in the development of cardiovascular disease, Nutr. J. 14 (1) (2015) 6.

[6] B. James, M. Meigs, F. Paul, P. Jacques, P. Jacob Selhub, E. Daniel, M. Singer, M. David, M. Nathan, P. Nader Rifai, et al., Fasting plasma homocysteine levels in the insulin resistance syndrome, Diabetes Care 24 (8) (2001) 1403–1410.
[7] M. Oron-Herman, T. Rosenthal, B.-A. Sela, Hyperhomocysteinemia as a component of syndrome X, Metabolism 52 (11) (2003) 1491–1495.
[8] Y. Li, C. Jiang, G. Xu, N. Wang, Y. Zhu, C. Tang, et al., Homocysteine upregulates resistin production from adipocytes in vivo and in vitro, Diabetes 57 (4) (2008) 817–827.
[9] Y. Li, H. Zhang, C. Jiang, M. Xu, Y. Pang, J. Feng, et al., Hyperhomocysteinemia promotes insulin resistance by inducing endoplasmic reticulum stress in adipose tissue, J. Biol. Chem. 288 (14) (2013) 9583–9592.
[10] X. Hu, V. Cifarelli, S. Sun, O. Kuda, N.A. Abumrad, X. Su, Major role of adipocyte prostaglandin E2 in lipolysis-induced macrophage recruitment, J. Lipid Res. 57 (4) (2016) 663–673.
[11] T.S. Nielsen, N. Jessen, J.O. Jorgensen, N. Moller, S. Lund, Dissecting adipose tissue lipolysis: molecular regulation and implications for metabolic disease, J. Mol. Endocrinol. 52 (3) (2014) R199–R222.
[12] P. Morigny, M. Houssier, E. Mouisel, D. Langin, Adipocyte lipolysis and insulin resistance, Biochimie 125 (2016) 259–266.
[13] X. Dou, Y. Xia, J. Chen, Y. Qian, S. Li, X. Zhang, et al., Rectification of impaired adipose tissue methylation status and lipolytic response contributes to hepatoprotective effect of betaine in a mouse model of alcoholic liver disease, Br. J. Pharmacol. 171 (17) (2014) 4073–4086.
[14] J. Deng, S. Liu, L. Zou, C. Xu, B. Geng, G. Xu, Lipolysis response to endoplasmic reticulum stress in adipose cells, J. Biol. Chem. 287 (9) (2012) 6240–6249.
[15] A.K. Hauck, Y. Huang, A.V. Hertzel, D.A. Bernlohr, Adipose oxidative stress and protein carbonylation, J. Biol. Chem. 294 (2019) 1083–1088.
[16] J.E. Chambers, S.J. Marciniak, Cellular mechanisms of endoplasmic reticulum stress signaling in health and disease. 2. Protein misfolding and ER stress, Am. J. Physiol. Cell Physiol. 307 (8) (2014) C657–C670.
[17] B.P. Tu, J.S. Weissman, Oxidative protein folding in eukaryotes: mechanisms and consequences, J. Cell Biol. 164 (3) (2004) 341–346.
[18] L. Wang, X. Wang, C.C. Wang, Protein disulfide-isomerase, a folding catalyst and a redox-regulated chaperone, Free Radic. Biol. Med. 83 (2015) 305–313.
[19] H.G. Hansen, J.D. Schmidt, C.L. Soltoft, T. Ramming, H.M. Geertz-Hansen, B. Christensen, et al., Hyperactivity of the Ero1alpha oxidase elicits endoplasmic reticulum stress but no broad antioxidant response, J. Biol. Chem. 287 (47) (2012) 39513–39523.
[20] B.G. Wouters, M. Koritzinsky, Hypoxia signalling through mTOR and the unfolded protein response in cancer, Nat. Rev. Canc. 8 (11) (2008) 851–864.
[21] T. McGarry, M. Biniecka, D.J. Veale, U. Fearon, Hypoxia, oxidative stress and inflammation, Free Radic. Biol. Med. 125 (2018) 15–24.
[22] G. Lian, X. Li, L. Zhang, Y. Zhang, L. Sun, X. Zhang, et al., Macrophage metabolic reprogramming aggravates aortic dissection through the HIF1alpha-ADAM17 pathway, EBioMedicine 49 (2019) 291–304.
[23] C. Jiang, A. Qu, T. Matsubara, T. Chanturiya, W. Jou, O. Gavrilova, et al., Disruption of hypoxia-inducible factor 1 in adipocytes improves insulin sensitivity and decreases adiposity in high-fat diet-fed mice, Diabetes 60 (10) (2011) 2484–2495.
[24] X. Wu, L. Zhang, Y. Miao, J. Yang, X. Wang, C-c Wang, et al., Homocysteine causes vascular endothelial dysfunction by disrupting endoplasmic reticulum redox homeostasis, Redox Biology 20 (2019) 46–59.
[25] Tomita S, Ueno M, Sakamoto M, Kitahama Y, Ueki M, Maekawa N, et al. Defective brain development in mice lacking the hif-1a gene in neural cells. Mol. Cell Biol..23 (19):6739-6749.
[26] W.Y. Kim, M. Safran, M.R.M. Buckley, B.L. Ebert, W.G. Kaelin, Failure to prolyl hydroxylate hypoxia-inducible factor α phenocopies VHL inactivation in vivo, EMBO J. 25 (19) (2006) 4650–4662.
[27] X. Xue, S. Ramakrishnan, E. Anderson, M. Taylor, E.M. Zimmermann, J.R. Spence, et al., Endothelial PAS domain protein 1 activates the inflammatory response in the intestinal epithelium to promote colitis in mice, Gastroenterology 145 (4) (2013) 831–841.
[28] C. Jiang, J.H. Kim, F. Li, A. Qu, O. Gavrilova, Y.M. Shah, et al., Hypoxia-inducible factor 1 regulates a SOCS3-STAT3-adiponectin signal transduction pathway in adipocytes, J. Biol. Chem. 288 (6) (2013), 3844-3857.
[29] Y. Fu, X. Wang, W. Kong, Hyperhomocysteinaemia and vascular injury: advances in mechanisms and drug targets, Br. J. Pharmacol. 175 (8) (2018) 1173–1189.
[30] A.N. Yang, H.P. Zhang, Y. Sun, X.L. Yang, N. Wang, G. Zhu, et al., High-methionine diets accelerate atherosclerosis by HHcy-mediated FABP4 gene demethylation pathway via DNMT1 in ApoE(-/-) mice, FEBS Lett. 589 (24 Pt B) (2015) 3998–4009.
[31] B. Meng, W. Gao, J. Wei, L. Pu, Z. Tang, C. Guo, Quercetin increases hepatic homocysteine remethylation and transsulfuration in rats fed a methionine-enriched diet, BioMed Res. Int. 2015 (2015) 815210.
[32] M. Schweiger, R. Schreiber, G. Haemmerle, A. Lass, C. Fledelius, P. Jacobsen, et al., Adipose triglyceride lipase and hormone-sensitive lipase are the major enzymes in adipose tissue triacylglycerol catabolism, J. Biol. Chem. 281 (52) (2006) 40236–40241.
[33] R. Zechner, R. Zimmermann, T.O. Eichmann, S.D. Kohlwein, G. Haemmerle, A. Lass, et al., FAT SIGNALS–lipases and lipolysis in lipid metabolism and signaling, Cell Metabol. 15 (3) (2012) 279–291.
[34] E. Bogdanovic, N. Kraus, D. Patsouris, L. Diao, V. Wang, A. Abdullahi, et al., Endoplasmic reticulum stress in adipose tissue augments lipolysis, J. Cell Mol. Med. 19 (1) (2015) 82–91.
[35] J. Li, J. Huang, J.S. Li, H. Chen, K. Huang, L. Zheng, Accumulation of endoplasmic reticulum stress and lipogenesis in the liver through generational effects of high fat diets, J. Hepatol. 56 (4) (2012) 900–907.
[36] M.R. Pulido, A. Diaz-Ruiz, Y. Jimenez-Gomez, S. Garcia-Navarro, F. Gracia-Navarro, F. Tinahones, et al., Rab18 dynamics in adipocytes in relation to lipogenesis, lipolysis and obesity, PloS One 6 (7) (2011), e22931.
[37] D. Xu, Y. Li, L. Wu, Y. Li, D. Zhao, J. Yu, et al., Rab18 promotes lipid droplet (LD) growth by tethering the ER to LDs through SNARE and NRZ interactions, J. Cell Biol. 217 (3) (2018) 975–995.
[38] K. Terai, Y. Hiramoto, M. Masaki, S. Sugiyama, T. Kuroda, M. Hori, et al., AMP-activated protein kinase protects cardiomyocytes against hypoxic injury through attenuation of endoplasmic reticulum stress, Mol. Cell Biol. 25 (21) (2005) 9554–9575.
[39] A. Kosteli, E. Sugaru, G. Haemmerle, J.F. Martin, J. Lei, R. Zechner, et al., Weight loss and lipolysis promote a dynamic immune response in murine adipose tissue, J. Clin. Invest. 120 (10) (2010) 3466–3479.
[40] S.Y. Zhang, Y.Q. Dong, P. Wang, X. Zhang, Y. Yan, L. Sun, et al., Adipocyte-derived lysophosphatidylcholine activates adipocyte and adipose tissue macrophage nod-like receptor protein 3 inflammasomes mediating homocysteine-induced insulin resistance, EBioMedicine 31 (2018) 202–216.
[41] J.G. Fan, J. Zhu, X.J. Li, L. Chen, L. Li, F. Dai, et al., Prevalence of and risk factors for fatty liver in a general population of Shanghai, China, J. Hepatol. 43 (3) (2005) 508–514.
[42] L. Yao, C. Wang, X. Zhang, L. Peng, W. Liu, X. Zhang, et al., Hyperhomocysteinemia activates the aryl hydrocarbon receptor/CD36 pathway to promote hepatic steatosis in mice, Hepatology 64 (1) (2016) 92–105.
[43] Hakan, Fotbolcu, Elcin, Zorlu. Nonalcoholic fatty liver disease as a multi-systemic disease. World J. Gastroenterol.. (16):4079-4090.
[44] M. Trauner, M. Arrese, M. Wagner, Fatty liver and lipotoxicity (3) (1801) 300–310.
[45] Z. Chen, R. Yu, Y. Xiong, F. Du, S. Zhu, A vicious circle between insulin resistance and inflammation in nonalcoholic fatty liver disease, Lipids Health Dis. 16 (1) (2017) 203.
[46] Z.G. Wang, X.B. Dou, Z.X. Zhou, Z.Y. Song, Adipose tissue-liver axis in alcoholic liver disease, World J. Gastrointest. Pathophysiol. 7 (1) (2016) 17–26.
[47] A.W. Christie, D.K.T. Mccormick, N. Emmison, F.B. Kraemer, K.G.M.M. Alberti, S. J. Yeaman, Mechanism of anti-lipolytic action of acipimox in isolated rat adipocytes, Diabetologia 39 (1) (1996) 45–53.
[48] B. Ahrén, Reducing plasma free fatty acids by acipimox improves glucose tolerance in high-fat fed mice, Acta Physiol. Scand. 171 (2) (2001) 161–167.
[49] Y. Wu, P. Song, W. Zhang, J. Liu, X. Dai, Z. Liu, et al., Activation of AMPKalpha2 in adipocytes is essential for nicotine-induced insulin resistance in vivo, Nat. Med. 21 (4) (2015) 373–382.
[50] Q. Long, X. Zhu, Y. Wu, B. Feng, D. Jin, J. Huang, et al., Molecular cloning and characterization of the porcine Ero1L and ERp44 genes: potential roles in controlling energy metabolism, Gen. Comp. Endocrinol. 173 (2) (2011) 259–269.
[51] Hudson DA, Gannon SA, Thorpe C. Oxidative protein folding: from thiol–disulfide exchange reactions to the redox poise of the endoplasmic reticulum. Free Radical Biol. Med..80:171-182.
[52] L. Wang, S.J. Li, A. Sidhu, L. Zhu, Y. Liang, R.B. Freedman, et al., Reconstitution of human Ero1-Lalpha/protein-disulfide isomerase oxidative folding pathway in vitro. Position-dependent differences in role between the a and a' domains of protein-disulfide isomerase, J. Biol. Chem. 284 (1) (2009) 199–206.
[53] D. Eletto, E. Chevet, Y. Argon, C. Appenzeller-Herzog, Redox controls UPR to control redox, J. Cell Sci. 127 (Pt 17) (2014) 3649–3658.
[54] Q.G. Zhou, M. Zhou, F.F. Hou, X. Peng, Asymmetrical dimethylarginine triggers lipolysis and inflammatory response via induction of endoplasmic reticulum stress in cultured adipocytes, Am. J. Physiol. Endocrinol. Metab. 296 (4) (2009) E869–E878.
[55] M. Gao, X. Huang, B.L. Song, H. Yang, The biogenesis of lipid droplets: lipids take center stage, Prog. Lipid Res. 75 (2019) 100989.
[56] B. Kong, T. Cheng, W. Wu, I. Regel, C.W. Michalski, Hypoxia-induced endoplasmic reticulum stress characterizes a necrotic phenotype of pancreatic cancer, Oncotarget 6 (31) (2015) 32154–32160.
[57] M.d V.E. Ortega, X. Xu, J. Koska, et al., Macrophage content in subcutaneous adipose tissue: associations with adiposity, age, inflammatory markers, and whole-body insulin action in healthy Pima Indians, Diabetes. 58 (2) (2009) 385–393.

Abbreviations

AMP: Adenosine monophosphate
Atf: Activating transcriptional factor
Atgl: Adipose triglyceride lipase
BAT: Brown adipose tissue
Bip: Binding protein
Cd36: Cluster of differentiation 36
CGI-58: Comparative gene identification-58
Chop: C/EBP homologous protein
DG: Diacylglycerol
Dgat: Diacylglycerol acyltransferase
ER: Endoplasmic reticulum
ERO1α: Endoplasmic reticulum oxidoreductin 1α
eWAT: epididymal white adipose tissue
FFAs: Free fatty acids
Hcy: Homocysteine
HHcy: Hyperhomocysteinemia

HIF1α: Hypoxia-inducible factor 1α
HMD: High-methionine diet
HRE: Hypoxia response element
Hsl: Hormone-sensitive lipase
IRE1: Inositol-requiring ER-to-nucleus signal kinase 1
LD: Lipid droplet
Mgl: Monoacylglycerol lipase
NAFL (D): Nonalcoholic fatty liver (disease)
Pdk1: Pyruvate dehydrogenase kinase isozyme 1
PERK: Protein kinase R-like ER kinase
PKA: Protein kinase A
Rab18: Ras-related protein 18
ROS: Reactive oxygen species
SAH: S-Adenosyl-L-homocysteine
SAM: S-Adenosylmethionine
scWAT: subcutaneous white adipose tissue
TC: Total cholesterol
TG: Triglyceride
UPR: Unfolded protein response